High-Performance Liquid Chromatography/High-Resolution Multiple Stage Tandem Mass Spectrometry Using Negative-Ion-Mode Hydroxide-Doped Electrospray Ionization for the Characterizat...

ARTICLE *in* ANALYTICAL CHEMISTRY · JUNE 2012

Impact Factor: 5.64 · DOI: 10.1021/ac300762y · Source: PubMed

analytical chemistry

Article

pubs.acs.org/ac

High-Performance Liquid Chromatography/High-Resolution Multiple Stage Tandem Mass Spectrometry Using Negative-Ion-Mode Hydroxide-Doped Electrospray Ionization for the Characterization of Lignin Degradation Products

Benjamin C. Owen,[†] Laura J. Haupert,[†] Tiffany M. Jarrell,[†] Christopher L. Marcum,[†] Trenton H. Parsell,[†] Mahdi M. Abu-Omar,[†] Joseph J. Bozell,[‡] Stuart K. Black,[§] and Hilkka I. Kenttämaa*[,†]

[†]Department of Chemistry, Purdue University, 560 Oval Drive, West Lafayette, Indiana 47907, United States

[‡]Center for Renewable Carbon, University of Tennessee, 2506 Jacob Drive, Knoxville, Tennessee 37996, United States

[§]National Renewable Energy Laboratory, 1617 Cole Boulevard, Golden, Colorado 80401, United States

Supporting Information

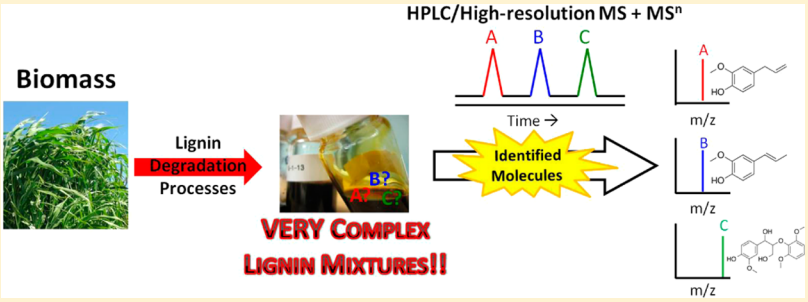

ABSTRACT: In the search for a replacement for fossil fuel and the valuable chemicals currently obtained from crude oil, lignocellulosic biomass has become a promising candidate as an alternative biorenewable source for crude oil. Hence, many research efforts focus on the extraction, degradation, and catalytic transformation of lignin, hemicellulose, and cellulose. Unfortunately, these processes result in the production of very complex mixtures. Further, while methods have been developed for the analysis of mixtures of oligosaccharides, this is not true for the complex mixtures generated upon degradation of lignin. For example, high-performance liquid chromatography/multiple stage tandem mass spectrometry (HPLC/MSⁿ), a tool proven to be invaluable in the analysis of complex mixtures derived from many other biopolymers, such as proteins and DNA, has not been implemented for lignin degradation products. In this study, we have developed an HPLC separation method for lignin degradation products that is amenable to negative-ion-mode electrospray ionization (ESI doped with NaOH), the best method identified thus far for ionization of lignin-related model compounds without fragmentation. The separated and ionized compounds are then analyzed by MS^3 experiments to obtain detailed structural information while simultaneously performing high-resolution measurements to determine their elemental compositions in the two parts of a commercial linear quadrupole ion trap/Fourier-transform ion cyclotron resonance mass spectrometer. A lignin degradation product mixture was analyzed using this method, and molecular structures were proposed for some components. This methodology significantly improves the ability to analyze complex product mixtures that result from degraded lignin.

With the advent of the energy crisis, lignocellulosic biomass has become of great interest for its potential to provide a biorenewable source for liquid transportation fuel and various valuable chemicals that are both currently derived from crude oil.[1−7] Lignin is a complex biopolymer of phenolic compounds found in plants. It is formed via free-radical polymerization of monomeric subunits called monolignols, the most common ones being *p*-coumaryl alcohol (H-unit in lignin), coniferyl alcohol (G-unit in lignin), and sinapyl alcohol (S-unit in lignin).[3,6−11] Lignin has a complex molecular network with diverse structural motifs. Its high oxygen content hinders the use of its degradation products as a fuel for transportation needs.[2,6,9] However, lignin has been found to have an energy content similar to that of coal.[12] To harness this energy, various extraction, degradation, and catalytic transformation processes are being explored for lignin.[3,6,9,10,13,14] Testing the usefulness of these processes requires analytical methods that can be used to characterize rapidly the complex mixtures produced.[15]

Multiple stage tandem mass spectrometry (MS^n) is a powerful technique for the direct analysis of many mixtures.[16−18] Mass spectrometry is capable of providing the

Received: March 22, 2012
Accepted: June 13, 2012
Published: June 13, 2012

   dx.doi.org/10.1021/ac300762y | *Anal. Chem.* 2012, 84, 6000−6007

molecular weights and, at high resolution, elemental compositions of unknown components in complex mixtures. MS^n provides molecular-level structural information for individual components of complex mixtures.[16−20] Collision-activated dissociation (CAD) is the most common method used to examine the structures of isolated ions in MS^n.[21−23] The onset of atmospheric pressure ionization sources, such as electrospray ionization (ESI), allowed for the coupling of MS detection and MS^n analysis to high-performance liquid chromatography (HPLC), thus adding a separation step to the analysis.[24−26] Recently, HPLC/MS^n has been demonstrated to be an invaluable tool for the analysis of complex mixtures derived from certain biopolymers.[27,28] However, this technique has yet to be implemented to the characterization of lignin degradation products.

Past efforts on reversed-phase HPLC separation of lignin degradation products have used multiangle laser light scattering,[29] diode array,[30,31] and electrochemical[32] methods for the detection of the analytes. Using these detectors prevents the identification of any previously unknown compounds. Furthermore, these methods are not amenable to detection by MS as the HPLC eluents consist of buffers incompatible with atmospheric pressure ionization specifically those containing nonvolatile salts.[29−32]

Recently, reversed-phase HPLC has been coupled with positive-ion-mode electron impact (EI) ionization and chemical ionization (CI),[33] thermospray[34,35] (TSP) ionization, fast atom bombardment[35] (FAB) ionization, and atmospheric pressure chemical ionization[36−39] (APCI) as well as ESI[36,40] mass spectrometry for the analysis of lignin degradation products. Unfortunately, none of these ionization methods are suitable for the analysis of unknown lignin degradation products in mixtures. EI and CI (carried out by using protonated water and acetonitrile as the CI reagent ions) were shown to cause massive fragmentation of the analytes,[33] while TSP, FAB, and APCI introduced significant biases by the preferential ionization of certain analytes in addition to causing massive fragmentation of the ionized analytes.[34−39] When using positive-ion-mode ESI, only the most basic compounds were detected.[40] Furthermore, when normal-phase HPLC separation was employed, ionization of the analytes by ESI was not possible because of the incompatibility of the nonpolar eluents with ESI.

Efficient ionization without fragmentation of all molecules in a mixture is arguably the most important step in mass spectrometric analyses of complex mixtures in order to ensure that all components of the mixture are identified. To date, the best ionization method found for lignin degradation products is negative-ion-mode ESI with NaOH dopant.[41] However, no HPLC methods have been reported in the literature for lignin degradation products that are amenable to negative-ion-mode ESI.[29−40]

The coupling of HPLC with negative-ion-mode high-resolution MS^3 analysis for the characterization of lignin degradation products is demonstrated in the present study. A solvent gradient system suitable for negative-ion-mode ESI was identified for the HPLC separation of model compounds. Sodium hydroxide was used as a dopant to facilitate the generation of stable deprotonated analytes. This methodology, combined with high-resolution MS^n, was utilized to provide structural information for components of a real lignin degradation mixture.

EXPERIMENTAL SECTION

Materials. Isoeguenol, eugenol, 2-methoxy-4-propylphenol, guaiacol, vanillin, vanillyl alcohol (all greater than 98% purity), ammonium acetate (>99% purity), and sinapyl alcohol (80% purity) were purchased from Sigma-Aldrich (St. Louis, MO). Coniferyl alcohol (98% purity) was purchased from Alfa-Aesar (Ward Hill, MA). 2-Methoxy-4-methylphenol (98% purity) and guaiacylglycerol-β-guaiacyl ether (99% purity) were obtained from TCI America (Portland, OR). Guaiacylglycerol-β-syringyl ether was synthesized by a previously published procedure that yields a mixture of diastereomers.[42] High-performance liquid chromatography−mass spectrometry (HPLC/MS) grade water, methanol and acetonitrile were purchased from Fisher Scientific (Pittsburgh, PA). All chemicals were used without further purification.

A Zorbax SB-C18 column (4.6 × 250 mm, 5 μm particle size) and a Zorbax SB-Phenyl column (4.6 × 250 mm, 5 μm particle size) were purchased from Agilent Technologies (Santa Clara, CA). A Kinetex PFP column (2.6 × 150 mm, 2.6 μm particle size) was purchased from Phenomenex (Torrance, CA).

Sample Preparation. Stock solutions were prepared for all analytes at a final concentration of 1.0 mM in 50/50 (v/v) methanol/water. For HPLC/MS analysis, the stock solutions were diluted (1:10) with 50/50 (v/v) methanol/water solution to achieve a final volume of 1 mL and an analyte concentration of 0.10 mM. To model a real lignin degradation product mixture, an artificial mixture of all the 12 model compounds studied was prepared by combining 100 μL of each stock solution, which yielded a final analyte concentration of about 0.090 mM and a sample volume of 1.1 mL.

A real lignin degradation product mixture was obtained by treating milled feedstock (red oak chips; 25 × 25 × 3 mm) in a flowthrough reactor with a 16:34:50 mixture of methyl isobutyl ketone:ethanol:water, respectively, at 140 °C in the presence of 0.05 M H_2SO_4 for 56 min. The resulting liquor contains mostly degraded lignin and hemicellulose, as cellulose is relatively insoluble in the extractant.[43] Additional water was added to the liquor to cause separation into an aqueous phase containing the hemicellulose degradation products and an organic phase containing the lignin degradation products. The solvent of the organic phase was removed under vacuum to give a degraded solid lignin residue. The solid was dissolved in 50/50 (v/v) methanol/water at a concentration of 4 mg/mL. For HPLC/MS, this solution was diluted by a factor of 2 with 50/50 (v/v) methanol/water for a final concentration of 2 mg/mL. This solution was analyzed by HPLC/MS^n.

Instrumentation. All experiments were performed using a Thermo Scientific linear quadrupole ion trap (LQIT)−Fourier transform ion cyclotron resonance (FT-ICR; 7 T magnet) mass spectrometer coupled with a Surveyor Plus high-performance liquid chromatograph consisting of a quaternary pump, autosampler, thermostatted column compartment, and photodiode array (PDA) detector. The mass spectrometer was equipped with an ESI source with a tee connector to mix the HPLC eluate with 10 mg/mL sodium hydroxide solution at a low flow rate (0.1 μL/min). This allows for efficient negative ion generation by ESI.[41] The LQIT-FT-ICR mass spectrometer was operated using the LTQ Tune Plus interface, and Xcalibur 2.0 software was used for HPLC/MS data analysis. The automated tuning feature of the instrument was used to optimize the measurements for low mass ions (m/z 50 to m/z

dx.doi.org/10.1021/ac300762y | Anal. Chem. 2012, 84, 6000−6007

500). AGC was used to ensure a stable ion signal. A nominal pressure of 0.60×10^{-5} Torr, as read by an ion gauge, was maintained in the higher pressure LQIT vacuum manifold and 2.0×10^{-10} Torr in the FT-ICR vacuum manifold, as read by an ion gauge.

High-Performance Liquid Chromatography/High-Resolution Tandem Mass Spectrometry. All samples were introduced into the HPLC/MS via an autosampler as a full-loop injection volume (three loop injection volumes (75 μL) + dead volume (17 μL) + wash volume (7.5 μL) = 99.5 μL) for high reproducibility. A 1 mg/L ammonium formate in water solution (A) and 1 mg/mL ammonium formate in acetonitrile solution (B) were used as the mobile phase solvents. Ammonium formate was chosen to encourage negative ion production.

Linear elution gradients were first optimized for each column examined by using a mix of the 12 model compounds with the elution occurring over 25 min at a constant flow rate of 0.5 mL/min. Different starting percentages of water and acetonitrile (from 95% A and 5% B to 75% A and 25% B) were tested by using the same ending percentages (5% A to 95% B) to achieve optimal separation. After an optimal linear gradient elution was identified, a nonlinear gradient, a two-slope gradient, elution were tested on each column by changing the gradient more rapidly in the last minute of elution (25% A and 75% B at 23.00 min to 5% A and 95% B at 24.00 min). All columns were equilibrated with the start eluent for 10 min before the next run. The columns were placed in a thermostatted column compartment that maintained the columns at a temperature of 30 °C to increase the reproducibility of the retention times and peak widths.

The PDA detector for HPLC was set at 214 nm. The conditions for ionization of the analytes and ion injection into the mass spectrometer were optimized using a stock solution of 2-methoxy-4-propylphenol in a 0.15 mg/mL NaOH 50:50 acetonitrile/water solution by employing the LTQ Tune Plus interface wherein all ion optics were optimized using the integrated tuning features. The ESI probe position was optimized manually for optimal signal. The following ESI conditions were used: sheath gas pressure 60 (arbitrary units), auxiliary gas pressure 30 (arbitrary units), sweep gas pressure 0 (arbitrary units), and spray voltage 3.50 kV.

Mass spectrometric detection of the pure model compounds in HPLC eluent was performed by ESI/MS. However, for the analysis of both artificial and real mixtures, data-dependent scans were used. Data-dependent scanning involves the instrument automatically selecting the most abundant ions (in this experiment, the three most abundant ions) from the ion source, one after each other, for further experiments. This allows for separate MS acquisitions to be performed simultaneously for the same ions in the two different mass analyzers of the LQIT-FT-ICR wherein the higher duty-cycle LQIT performs tandem mass spectral acquisitions for the selected ions while the lower duty-cycle FT-ICR carries out high-resolution measurements for elemental composition determination for the same ions. A resolving power of 400 000 at m/z 400 was used in the FT-ICR. The MS^2 experiments involve the isolation (using a mass/charge ratio window of 2 Th) and fragmentation of selected ions formed upon negative-ion-mode ESI. The ion abundance cutoff for performing CAD was determined by tripling the average abundance of background ions in the total ion current (TIC) collected when a methanol/water solution (50/50; v/v) was injected into the column. The ions were kinetically excited and allowed to undergo collisions with helium target gas for 30 ms at a q value of 0.25 (a parameter in the Matthieu stability diagram that determines which sizes of ions are trapped as well as the initial kinetic energy of the ion subjected to CAD) at a normalized collision energy[20] of 40%. The most abundant product ion formed in the MS^2 experiments was subjected to a further stage of ion isolation and fragmentation (MS^3). Fragmentation products having at least 5% abundance relative to the most abundant product ion are reported.

RESULTS AND DISCUSSION

To develop and assess an HPLC/MS^n analysis method for lignin degradation products, pure standard solutions as well as a mixture of 12 model compounds of lignin degradation products (Table 1) were subjected to separation by reversed-phase HPLC using an acetonitrile and water gradient elution followed by high-resolution MS^3 analysis. Three reversed-phase HPLC columns were chosen for testing the separation of the model compound mixture: a Zorbax SB-C18 (chosen for its common use in HPLC separation), a Zorbax SB-Phenyl (chosen because of its efficiency in separating substituted aromatic compounds) and a Kinetex PFP (chosen because of its efficiency in separating compounds having different polar or halogenated substituents on a phenyl ring). A solvent gradient system was

Table 1. Chromatographic Separation of a Mixture of Model Compounds by Using Zorbax SB-C18, Zorbax SB-Phenyl, and Kinetex PFP Columns

Model Compound (m/z of $[M-H]^-$; Determined Elemental Composition)	Measured Exact m/z (error in ±mTh from the expected exact mass)
[A] Guaiacol (123; $C_7H_7O_2$) 	123.0458 (1.2)
[B] 2-Methoxy-4-methylphenol (137; $C_8H_9O_2$) 	137.0615 (1.3)
[C] Vanillin (151; $C_8H_7O_3$) 	151.0408 (1.3)
[D] Vanillyl alcohol (153; $C_8H_9O_3$) 	153.0564 (1.2)
[E] Eugenol (163; $C_{10}H_{11}O_2$) 	163.0771 (1.2)
[F] Isoeugenol (163; $C_{10}H_{11}O_2$) 	163.0771 (1.2)
[G] 2-Methoxy-4-propylphenol (165; $C_{10}H_{13}O_2$) 	165.0927 (1.2)
[H] Coniferyl alcohol (179; $C_{10}H_{11}O_3$) 	179.0717 (0.9)
[I] Sinapyl alcohol (209; $C_{11}H_{13}O_4$) 	209.0819 (0.5)
[J] Guaiacylglycerol-β-guaiacylether (319; $C_{17}H_{19}O_6$) 	319.1186 (0.4)
[K+L] Guaiacylglycerol-β-syringylether stereoisomers (349; $C_{18}H_{21}O_7$) 	349.1292 (0.5)

dx.doi.org/10.1021/ac300762y | Anal. Chem. 2012, 84, 6000−6007

developed by testing several buffer salts and their concentrations in the mobile phase. This was necessary, as all current HPLC methodologies developed for lignin degradation products used nonvolatile buffers and/or acidic mobile phases that are incompatible with negative-ion-mode ESI detection.[29−40] After testing multiple MS-compatible buffers, ammonium formate was found to be the optimal buffer. At a concentration of 1 mg/mL, this buffer generated a stable ESI spray with and without NaOH dopant at a low spray current that is needed to prevent arcing.

Analytes eluting from the HPLC were detected by UV light absorbance by using the PDA detector and by detecting all the ions (a total ion chromatogram, TIC) generated upon ESI in the mass spectrometer during the HPLC run. In addition to the acquisition of high-resolution mass spectra for the compounds eluting from HPLC (MS^1), ions formed from these compounds were subjected to isolation and CAD experiments until no further fragmentation products were observed (up to MS^3). A detailed discussion of the results obtained for the three different columns by using model compounds and their equimolar mixture is given below, together, with results obtained for the degradation products of a real lignin sample.

Zorbax SB-C18 Column. The Zorbax SB-C18 is a reversed-phase HPLC column packed with porous silica microspheres that are functionalized with a sterically protected diisobutyl-*n*-octadecylsilane stationary phase. The optimal gradient elution for this column was determined to be nonlinear: 0.00 min, 80% A and 20% B; 23.00 min, 25% A and 75% B; 24.00 min, 5% A and 95% B; 24.99 min, 5% A and 95% B; 25.00 min, 80% A and 20% B; 35.00 min (10.00 min re-equilibration time), 80% A and 20% B. The retention times for the model compounds, as observed for the stock solutions and an artificial mixture containing an equimolar concentration of all the model compounds studied, are given in Table S-1 (Supporting Information). Figure S-1 (Supporting Information) shows the UV chromatogram and extracted ion chromatogram (XIC), which was obtained after the separation by a data-mining process wherein the deprotonated model compounds' abundances are plotted as a function of time for the model mixture. The polarities of the analytes were found to have the largest effect on the retention times, as expected.[44] Highly polar benzyl alcohols eluted first, followed by the compounds with the allylic alcohol moiety. The last compound to elute was 4-methoxypropylphenol, the least polar model compound studied. Despite their large size, compounds with many oxygens, such as the dimers, had retention times shorter than those of smaller nonpolar molecules. In addition to the degree of oxidation, the lengths of alkyl chains and their saturation level also play a role in the chromatographic separation of the model compounds. This can be seen in the following elution order: guaiacol (no alkyl groups), 2-methoxy-4-methylphenol (methyl group), eugenol (allyl group), isoeugenol (1-propenyl group), and 2-methoxy-4-propylphenol (propyl group) (see Figure S-1). This elution order indicates that the longer and more saturated the alkyl chain in a molecule, the more time it spends in the column. All model compounds were separated in this column.

Zorbax SB-Phenyl Column. The Zorbax SB-Phenyl column is also a reversed-phase HPLC column. It is packed with porous silica microspheres that are functionalized with a sterically protected diisopropyl-2-phenylethylsilane stationary phase. The optimal nonlinear gradient elution for this column: 0.00 min, 80% A and 20% B; 23.00 min, 25% A and 75% B; 24.00 min, 5% A and 95% B; 24.99 min, 5% A and 95% B; 25.00 min, 80% A and 20% B; 35.00 min (10.00 min re-equilibration time), 80% A and 20% B. The retention times for the model compounds, as observed for the stock solutions and the model mixture, are given in Table S-1. Figure 1 shows the

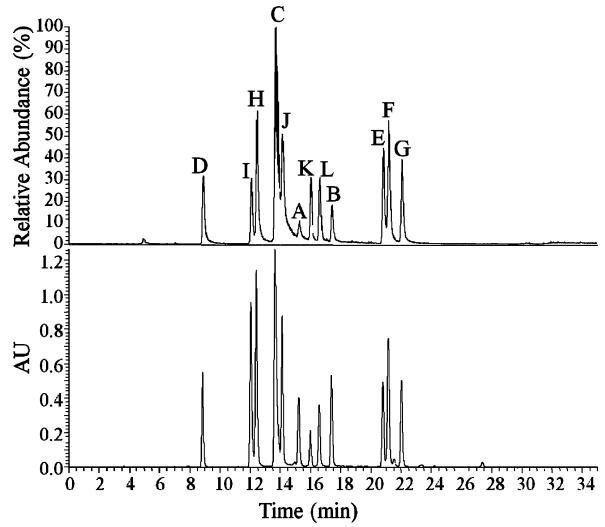

Figure 1. The selected ion chromatogram for the deprotonated compounds (top) and the UV absorbance chromatogram (in absorbance units (AU); bottom) for the HPLC separation of a mixture of 12 model compounds on the Zorbax SB-Phenyl column.

UV chromatogram and XIC for the deprotonated compounds in the model mixture. The polarities of the analytes were found to have the largest effect on their elution times, as expected,[44] with the earliest eluting compounds being vanillyl alcohol (first), sinapyl alcohol (second), and coniferyl alcohol (third). The last compound to elute was 4-methoxypropylphenol, the least polar model compound studied. Also, the degree and type of substitution on the phenyl rings has been reported to play an important role for this column.[44] This effect is indicated, for example, by the earlier elution of guaiacol (a monosubstituted *o*-methoxyphenol) relative to the more polar guaiacylglycerol-*β*-syringyl ether diastereomers that are larger and have three methoxy substituents. Hence, the smaller but less polar analyte eluted before the larger and more polar analytes, as opposed to what was observed for the C18 column.[44] Moreover, 2-methoxy-4-methylphenol elutes with a similar retention time compared to the more polar guaiacylglycerol-*β*-syringyl ether diastereomers, which supports the notion[44] that the degree of polarity has a larger effect on separation than the number and length of alkyl groups.

The elution time difference between guaiacol and 2-methoxy-4-methylphenol in the SB-Phenyl column, when compared to the SB-C18 column, was a minute shorter. This result suggests a lower separation efficiency in the SB-Phenyl column for alkyl-substituted analytes with a different number of alkyl groups. However, the benefit of using the Zorbax SB-Phenyl column is its ability to separate a wider range of analytes with varying polarities. It took 5 min for the most polar analyte, vanillyl alcohol, to elute from the SB-Phenyl column and 18.2 min for the least polar analyte, 2-methoxy-4-propylphenol to elute. Having extra time in the gradient before and after the elution of the model compounds studied could allow for the elution of both more and less polar compounds. All model compounds were separated in this column.

dx.doi.org/10.1021/ac300762y | *Anal. Chem.* 2012, 84, 6000−6007

Kinetex PFP Column. The Kinetex PFP column is a reversed-phase HPLC column packed with core−shell silica microspheres (nonporous silica core with a porous silica shell) that are functionalized with a pentafluorophenyl stationary phase. The optimal linear gradient elution for this column is: 0.00 min, 80% A and 20% B; 23.00 min, 5% A and 95% B; 24.99 min, 5% A and 95% B; 25.00 min, 80% A and 20% B; 35.00 min (10.00 min re-equilibration time), 80% A and 20% B. The retention times for the model compounds, as observed for the stock solutions and the model mixture, are given in Table S-1. Figure S-2 (Supporting Information) shows the UV chromatogram and XIC for the deprotonated model compounds in the model mixture. Overall, this column resulted in the poorest separation of the model compounds. While maintaining the same separation profile as the Zorbax SB-Phenyl column, with the exception of the earlier elution of guaiacylglycerol-β-guaiacyl ether, the PFP column failed to fully separate coniferyl alcohol, sinapyl alcohol, guaiacol, and guaiacylglycerol-β-syringyl ether diastereomers. The eluted peaks were significantly widened compared to the other two columns, and the determination of the retention times had a higher degree of uncertainty. However, the benefit of this column is that it could separate nonpolar compounds and avoid the retention of more nonpolar analytes in the column, as indicated by the earlier elution of the least polar compound studied, 2-methoxy-4-propylphenol (13.52 min), when compared to the Zorbax SB-C18 column (24.59 min). The above effects are due to the more polar stationary phase of this column than the other two, as well as the higher column backpressure.

High-Resolution Mass Spectrometry and Tandem Mass Spectrometry. All model compounds produced exclusively a stable and abundant deprotonated molecule, $[M - H]^-$, upon negative-ion-mode ESI with NaOH dopant. The $[M - H]^-$ ions allow for the determination of the molecular weights and elemental compositions for unknown compounds, as demonstrated for the components of the model compound mixture after HPLC separation (Table 1; Table S-1). The errors (in ±mTh) reported for the exact mass measurements (Table 1; Table S-1) were obtained from full mass spectral acquisitions for ions with m/z values from 50 − 500.

When examining pure model compounds, were acquired mass spectra in the LQIT to determine the retention time for each molecule (Table S-1). However, for mixtures, data-dependent analysis was performed. In these analyses, a scan function was utilized that first carried out a low-resolution FT-ICR acquisition to make decisions about the MS^2 experiments to be performed in the LQIT. The FT-ICR transient was Fourier-transformed at an acquisition time that achieves 25 000 resolving power to identify the three most abundant ions in each mass spectrum (with a normalized abundance greater than 5×10^6 intensity units) to be subjected to CAD in the LQIT (Table S-2 (Supporting Information)). The most abundant product ion formed in each of these MS^2 experiments was subjected to a further stage of ion isolation and CAD (MS^3; Table S-2) to explore the extent of structural information attainable from these experiments. While the LQIT performed these MS^3 experiments, the FT-ICR was simultaneously continuing the acquisition of the same transient, as previously, for a longer time to achieve 400 000 resolving power that allows a more accurate exact mass measurement.

All model compounds with methoxy substituents attached to an aromatic ring fragmented by the loss of a methyl radical via a homolytic cleavage of an oxygen−methyl bond. Additionally, all ions containing allylic or benzylic hydroxy functionalities (vanillyl alcohol, coniferyl alcohol, and sinapyl alcohol) fragmented primarily by loss of water. However, for the deprotonated sinapyl alcohol, the loss of a methyl radical was even more dominant. This observation can be explained by the presence of two methoxy groups in this molecule. Thus, it contains two sites that are equally likely to lose a methyl radical. The deprotonated guaiacylglycerol-β-guaiacyl ether predominantly lost water followed by loss of formaldehyde, fragmentations characteristic of a β-aryl ether linkage in lignin.[45] The loss of water is initiated by the cleavage of the benzylic hydroxyl group as a hydroxide ion that subsequently deprotonates the primary hydroxyl group in the β-aryl ether moiety (Scheme S-1 (Supporting Information)).[45] The primary alkoxide ion formed in this fragmentation is cleaved off as formaldehyde, allowing for the negative charge to be delocalized. Another product ion observed for deprotonated guaiacylglycerol-β-guaiacyl ether was formed by a loss of guaiacol, thus revealing the presence of a G-subunit in this molecule.

The diastereomer pairs (*RS*/*SR* and *RR*/*SS*) of guaiacylglycerol-β-syringyl ether were successfully separated by HPLC, and though all of the same ionic fragmentation products were observed for the deprotonated diastereomer pairs, the relative abundances of the product ions were vastly different. One deprotonated diastereomer pair fragmented by facile loss of water and subsequent loss of formaldehyde (analogous to the fragmentation observed for deprotonated guaiacylglycerol-β-guaiacyl ether), while the other deprotonated diasteriomer pair predominantly lost syringol (S-unit), which is analogous to the guaiacol loss observed for deprotonated guaiacylglycerol-β-guaiacyl ether. Further mechanistic investigations are needed to identify which deprotonated diastereomer pair (*RS*/*SR* and *RR*/*SS*) predominantly loses water and which loses syringol.

To explore whether further structural information can be obtained from MS^3 experiments, the most abundant product ion formed in the MS^2 experiment was isolated and subjected to CAD (Table S-2). For some ions that lack a weakly bound group, no further fragmentation was observed. However, most of the ions fragmented to yield structurally informative product ions not observed in the MS^2 experiments, which demonstrates that the use of multiple-stage tandem mass spectrometry is useful in the structural characterization of unknown lignin degradation products.

Deprotonated sinapyl alcohol that contains two methoxy groups lost a methyl radical in the MS^2 experiment followed by another methyl radical loss in the MS^3 experiment, which allows for the counting of the methoxy substituents in this analyte. In the case of deprotonated 2-methoxy-4-propylphenol, the product ion formed by methyl radical loss in the MS^2 experiment fragmented in the MS^3 experiment by loss of an ethyl radical through the homolytic cleavage of a benzylic bond, which reveals the presence of a propyl substituent. An analogous benzylic bond cleavage was also observed for deprotonated eugenol. The product ion formed by loss of a methyl radical from deprotonated eugenol fragments by the cleavage of a benzylic carbon−hydrogen bond to lose a hydrogen atom. In contrast, the ion formed upon loss of a methyl radical from deprotonated isoeugenol does not fragment further because of the lack of a weakly bound substituent. This difference in MS^3 fragmentation allows for the differentiation of these structural isomers.

dx.doi.org/10.1021/ac300762y | *Anal. Chem.* 2012, 84, 6000−6007

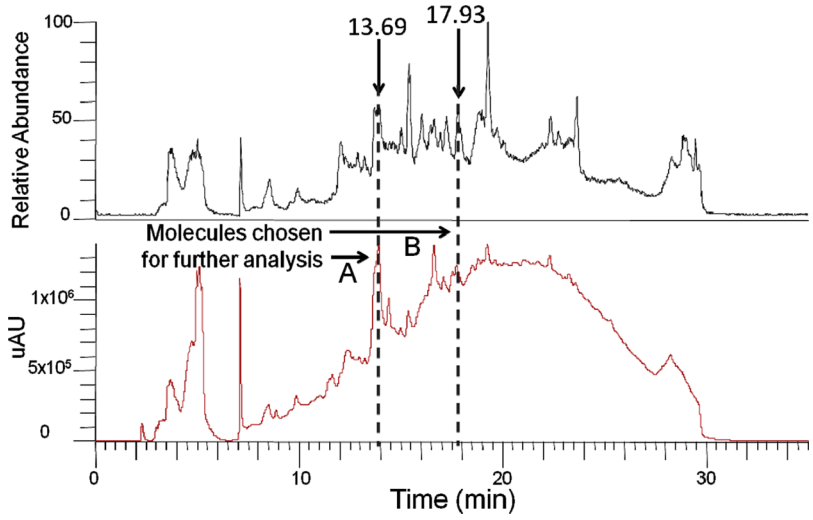

Figure 2. TIC (top) and UV absorbance (in absorbance units (AU); bottom) chromatograms for the HPLC separation of a degraded oak lignin sample on the SB-Phenyl column. (Note: Unknown molecules A and B chosen for further analysis).

The ions formed upon loss of water and formaldehyde from deprotonated guaiacylglycerol-β-guaiacyl ether and guaiacylglycerol-β-syringyl ether reveal the presence of a methoxy group through a facile methyl radical loss upon MS^3. The presence of the G- and S-units, respectively, in deprotonated guaiacylglycerol-β-guaiacyl ether and guaiacylglycerol-β-syringyl ether are revealed by the fragmentation of their product ions formed by loss of water and formaldehyde via the loss of a guaicyl radical (C_7H_7O; methoxyphenyl radical) and syringyl radical ($C_8H_9O_2$; dimethoxyphenyl radical), respectively, wherein the phenyl−oxygen bond is homolytically cleaved (Scheme S-2 (Supporting Information)). The major loss of CO_2 from the product ion formed by loss of a methyl radical from deprotonated vanillin is currently under investigation and will be discussed in future publications.

Lower Limit of Detection/Lower Limit of Quantitation for the HPLC/MS Method. To evaluate the lower limit of detection (LOD), lower limit of quantitation (LOQ), and lower limit of mass (in grams) detection (gLOD; defined as the smallest detectable mass (in grams) of sample injected onto the column), standard solutions of vanillin and 2-methoxy-4-propylphenol were separated on the Zorbax SB-Phenyl column and detected by mass spectrometry. The standard solutions were made from the 1.0 mM stock solutions discussed above and diluted to a final volume of 1.0 mL with the following concentrations of either vanillin or 2-methoxy-4-propylphenol: 0.010, 0.030, 0.050, 0.070, 0.10, 0.15, 0.30, 0.60, and 1.0 μM. 2-Methoxy-4-methylphenol was used as the internal standard (1.0 μM) and was added to all of the standard solutions. A full loop injection was performed for each standard solution; thus, a total volume of 25 μL was injected onto the column. After separation, the XICs for deprotonated vanillin and 2-methoxy-4-propylphenol were extracted by Thermo Xcalibur Quan Browser software and used to create the calibration curves. The LOD and LOQ were determined from the calibration curves by finding the point where the peak height measured for each analyte was greater than $3\sigma_{noise}$ and $10\sigma_{noise}$, respectively. The calibration curves are shown in Figure S-3 (Supporting Information) along with the reported LOD, LOQ, and gLOD values. For vanillin and 2-methoxy-4-propylphenol, the LOD was found to be 0.024 μM and 0.017 μM, the LOQ was 0.079 μM and 0.048 μM, and the gLOD was 40 pg and 20 pg, respectively. These values compare well with previous literature results obtained using similar HPLC/MS methods to separate cellulose biomass components using MS detection.[46] These analytical figures of merit ensure that the new method is able to detect all components in a complex mixture that have a concentration greater than 24 nM.

Identification of Unknown Compounds in a Lignin Degradation Product Mixture. To assess the ability of the above method to identify unknown components in lignin degradation product mixtures, an organsolv oak lignin residue was subjected to analysis by HPLC/MS using the Zorbax SB-Phenyl column. Though the organosolv lignin sample is a very complex mixture (Figure 2; Figure S-4 (Supporting Information)), HPLC was able to separate many analytes, including isobaric and isomeric molecules (Figure S-5 (Supporting Information)). Attaining this high-quality separation ensures the quality of MS^n experiments by avoiding the simultaneous isolation and dissociation of multiple species and complication of the CAD spectra. The data-dependent HPLC/MS^3 method described above (Experimental Section) was used to determine the exact m/z value and fragmentation patterns of eluting molecules after ionization.

The above experiments allow molecular structures to be proposed for the mixture components. For example, a molecule that strongly absorbs UV light (molecule denoted as "A" in Figure 2; retention time of 13.69 min) was determined to form a deprotonated molecule with an exact m/z value of 151.040 corresponding to an elemental composition of $C_8H_7O_3$ (with +1.4 mTh deviation from the expected value) and a double bond equivalent (DBE) of 5 (corresponding to a compound with one phenyl ring and one double bond or five double bonds).

Upon MS^2, the unknown deprotonated molecule fragmented via a methyl radical loss, which indicates that the molecule contains a methoxy group bound to an aromatic ring.[41,47] The product ion formed by methyl radical loss in the MS^2 experiment fragmented in the MS^3 experiment via a facile CO_2 loss (44 Da; 83%) and a less facile CO loss (28 Da; 17%). These fragmentations are identical to those of a deprotonated model compound studied here, vanillin (Figure S-6 (Supporting Information)). Also, the exact m/z value and DBE correspond to that of deprotonated vanillin. Finally, the

dx.doi.org/10.1021/ac300762y | Anal. Chem. 2012, 84, 6000−6007

Scheme 1. Proposed Mechanism for the Fragmentation Pathways of the Unknown Deprotonated Molecule of *m/z* 329 Leading to the Loss of Methyl Radical and an Ion of *m/z* 193

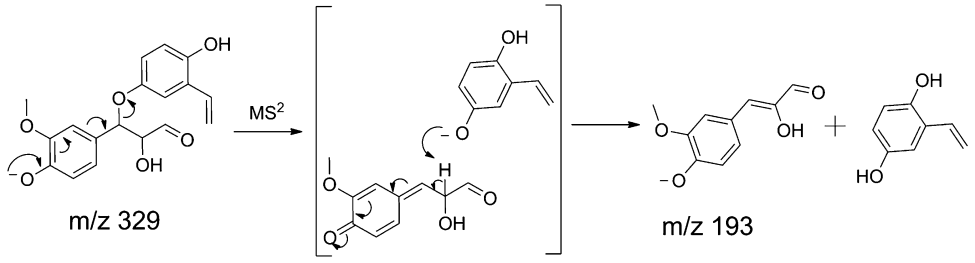

HPLC retention time of the unknown compound is similar to that of vanillin. Hence, this unknown compound in the lignin degradation product mixture is identified as vanillin.

The concentration of vanillin in the lignin degradation product solution was determined by generating a calibration curve by using standard solutions with vanillin concentrations of 0.500, 1.00, 5.00, 10.0, and 50.0 μM. 2-Methoxy-4-methylphenol was used as the internal standard (10.0 μM) and was added to the standard solutions and to the lignin degradation product solution. The vanillin concentration was found to be 0.043 mM in the lignin degradation product solution, indicating a mass percent of 0.16% of vanillin in the solid lignin degradation mixture.

As this molecule was a known model compound, a second molecule was proposed and a molecular structure was chosen. A molecule later in retention time than vanillin (molecule denoted as "B" in Figure 2; retention time of 17.93 min) was determined to form a deprotonated molecule with an exact *m/z* value of 329.1029 corresponding to an elemental composition of $C_{18}H_{17}O_6$ (with +0.4 mTh deviation from the expected value) and a double bond equivalent (DBE) of 10 (corresponding to a compound with two phenyl rings and two double bonds, one phenyl ring and 6 double bonds, or 10 double bonds with the first of the three choices being the most likely and indicative of a lignin-like structure; Figure S-7 (Supporting Information)).

Upon MS^2 (Figure S-8 (Supporting Information)), the unknown deprotonated molecule fragmented via a single methyl radical loss, which indicates that the molecule contains one methoxy group bound to an aromatic ring.[41,47] A second abundant MS^2 product ion (*m/z* 193) results from the loss of 136 from the deprotonated molecule, revealing that there are two subunits to this molecule connected by either a benzylic or other weak-type linkage as in the β-aryl ether linkage; however, the lack of a loss of formaldehyde occurring from the deprotonated molecule (*m/z* 329) eliminates the possibility of a β-aryl ether linkage and reveals that the subunits are connected by a benzylic ether linkage. The product ion formed from the loss of 136 in the MS^2 experiment (*m/z* 193) fragmented in the MS^3 experiment (Figure S-8) via a methyl radical loss (*m/z* 178), a CO loss (*m/z* 165), and successive CO and methyl radical losses (*m/z* 150). These fragmentation pathways indicate that the ion of *m/z* 193 subjected to MS^3 experiments contains the single methoxy group bound to an aromatic ring seen in the MS^2 experiment as well as a phenolic oxygen revealed by the loss of CO. From the aforementioned observations together with the presence of a doubly deprotonated molecule (*m/z* 164) in the MS^1 spectrum revealing the presence of two phenolic oxygens on different phenyl subunits (see Figure S-7 and S-9 (Supporting Information) for the support of these claims), the structural assignment of the ion of *m/z* 349 is straightforward (Scheme 1).

CONCLUSIONS

Three HPLC columns were examined for their ability to separate a mixture of 12 lignin-related model compounds. Using a water and acetonitrile gradient buffered with ammonium formate, full baseline separation was attained for all mixture components when using both the Zorbax SB-C18 and Zorbax SB-Phenyl column, while a poorer separation was attained for the Kinetex PFP column. High-resolution mass spectrometric detection of the eluent allowed for the exact *m/z* value measurement for the deprotonated mixture components. MS^2 and MS^3 experiments revealed structurally informative fragmentation patterns for the model compounds. It should be noted here that the MS^n experiments can be carried out much further than to the MS^3 level if so desired (up to MS^7 has been performed in our laboratories for a compound eluting from HPLC). The same methodology was used for the structural elucidation of an abundant molecule in a real lignin degradation product mixture. Furthermore, a low limit of detection, low limit of quantitation, and low gram limit of detection were determined. The ability to separate, identify, and quantify unknown components in complex mixtures will facilitate the efforts to convert biomass and, more specifically, lignin into valuable chemicals and transportation fuels that are currently obtained from crude oil.

ASSOCIATED CONTENT

Supporting Information

Additional information as noted in the text. This material is available free of charge via the Internet at http://pubs.acs.org.

AUTHOR INFORMATION

Corresponding Author

*Phone: (765) 494-0882; fax: (765) 494-0239; e-mail: hilkka@purdue.edu.

Notes

The authors declare no competing financial interest.

ACKNOWLEDGMENTS

This work was supported as part of the Center for Direct Catalytic Conversion of Biomass to Biofuels (C3Bio), an Energy Frontier Research Center funded by the U.S. Department of Energy, Office of Science, Office of Basic Energy Sciences under Award Number DE-SC0000997.

REFERENCES

(1) Chang, M. C. Y. *Curr. Opin. Chem. Biol.* **2007**, *11*, 677–684.

(2) Hamelinck, C. N.; van Hooijdonk, G.; Faaij, A. P. C. *Biomass Bioenergy* **2005**, *28*, 384−410.
(3) Hisano, H.; Nandakumar, R.; Wang, Z.-Y. *In Vitro Cell. Dev. Biol.: Plant* **2009**, *45*, 306−313.
(4) Mohan, D.; Pittman, C. U.; Steele, P. H. *Energy Fuels* **2006**, *20*, 848−889.
(5) Ragauskas, A. J.; Williams, C. K.; Davison, B. H.; Britovsek, G.; Cairney, J.; Eckert, C. A.; Frederick, W. J.; Hallett, J. P.; Leak, D. J.; Liotta, C. L.; Mielenz, J. R.; Murphy, R.; Templer, R.; Tschaplinski, T. *Science* **2006**, *311*, 484−489.
(6) Weng, J.-K.; Li, X.; Bonawitz, N. D.; Chapple, C. *Curr. Opin. Biotechnol.* **2008**, *19*, 166−172.
(7) Zakzeski, J.; Bruijnincx, P. C. A.; Jongerius, A. L.; Weckhuysen, B. M. *Chem. Rev.* **2010**, *110*, 3552−3599.
(8) Boerjan, W.; Ralph, J.; Baucher, M. *Annu. Rev. Plant Biol.* **2003**, *54*, 519−546.
(9) Cherubini, F.; Stromman, A. H. *Energy Fuels* **2010**, *24*, 2657−2666.
(10) Li, X.; Weng, J. K.; Chapple, C. *Plant J.* **2008**, *54*, 569−581.
(11) Ralph, J.; Lundquist, K.; Brunow, G.; Lu, F.; Kim, H.; Schatz, P. F.; Marita, J. M.; Hatfield, R. D.; Ralph, S. A.; Christensen, J. H.; Boerjan, W. *Phytochem. Rev.* **2004**, *3*, 29−60.
(12) McLaughlin, S. B.; Samson, R.; Bransby, D.; Wiselogel, A. *Bioenergy '96 Proc. Natl. Bioenergy Conf., 7th* **1996**.
(13) Hanson, S. K.; Baker, R. T.; Gordon, J. C.; Scott, B. L.; Thorn, D. L. *Inorg. Chem.* **2010**, *49*, 5611−5618.
(14) Hasegawa, I.; Inoue, Y.; Muranaka, Y.; Yasukawa, T.; Mae, K. *Energy Fuels* **2011**, *25*, 791−796.
(15) Brunow, G. In *Biopolymers*; Steinbüchel, A., Ed.; Wiley: New York, 2001; Vol. *1*, pp 89−99.
(16) Amy, J. W.; Baitinger, W. E.; Cooks, R. G. *J. Am. Soc. Mass Spectrom.* **1990**, *1*, 119−128.
(17) Cooks, R. G.; Busch, K. L.; Glish, G. L. *Science* **1983**, *222*, 273−291.
(18) McLafferty, F. W. *Int. J. Mass Spectrom.* **2001**, *212*, 81−87.
(19) Amundson, L. M.; Owen, B. C.; Gallardo, V. A.; Habicht, S. C.; Fu, M. K.; Shea, R. C.; Mossman, A. B.; Kenttämaa, H. I. *J. Am. Soc. Mass. Spectrom.* **2011**, *22*, 670−682.
(20) Lopez, L. L.; Tiller, P. R.; Senko, M. W.; Schwartz, J. C. *Rapid Commun. Mass Spectrom.* **1999**, *13*, 663−668.
(21) Mayer, P. M.; Poon, C. *Mass Spectrom. Rev.* **2009**, *28*, 608−639.
(22) McLuckey, S. A. *J. Am. Soc. Mass Spectrom.* **1992**, *3*, 599−614.
(23) Sleno, L.; Volmer, D. A. *J. Mass Spectrom.* **2004**, *39*, 1091−1112.
(24) Dole, M.; Mack, L. L.; Hines, R. L. *J. Chem. Phys.* **1968**, *49*, 2240−&.
(25) Fenn, J. B.; Mann, M.; Meng, C. K.; Wong, S. F.; Whitehouse, C. M. *Science* **1989**, *246*, 64−71.
(26) Yamashita, M.; Fenn, J. B. *J. Phys. Chem.* **1984**, *88*, 4451−4459.
(27) Domon, B.; Aebersold, R. *Science* **2006**, *312*, 212−217.
(28) Wysocki, V. H.; Resing, K. A.; Zhang, Q. F.; Cheng, G. L. *Methods* **2005**, *35*, 211−222.
(29) Gidh, A. V.; Decker, S. R.; Vinzant, T. B.; Himmel, M. E.; Williford, C. *J. Chromatogr., A* **2006**, *1114*, 102−110.
(30) Jiang, Z.; Zhu, J.; Li, X.; Lian, Z.; Yu, S.; Yong, Q. *Sepu* **2011**, *29*, 59−62.
(31) Lobbes, J. M.; Fitznar, H. P.; Kattner, G. *Anal. Chem.* **1999**, *71*, 3008−3012.
(32) Galletti, G. C.; Piccaglia, R.; Chiavari, G.; Concialini, V.; Buta, J. G. *Chromatographia* **1988**, *26*, 191−196.
(33) van der Hage, E. R. E.; Boon, J. J. *J. Chromatogr., A* **1996**, *736*, 61−75.
(34) Galletti, G. C.; Eagles, J.; Mellon, F. A. *J. Sci. Food Agric.* **1992**, *59*, 401−404.
(35) Mellon, F. A. *Liquid Chromatography/Mass Spectrometry and Fast Atom Bombardment Mass Spectrometry of Polyphenols*; Elsevier: New York, 1991.
(36) Damiani, I.; Morreel, K.; Danoun, S.; Goeminne, G.; Yahiaoui, N.; Marque, C.; Kopka, J.; Messens, E.; Goffner, D.; Boerjan, W.; Boudet, A. M.; Rochange, S. *Plant Mol. Biol.* **2005**, *59*, 753−769.
(37) Morreel, K.; Ralph, J.; Kim, H.; Lu, F. C.; Goeminne, G.; Ralph, S.; Messens, E.; Boerjan, W. *Plant Physiol.* **2004**, *136*, 3537−3549.
(38) Morreel, K.; Ralph, J.; Lu, F. C.; Goeminne, G.; Busson, R.; Herdewijn, P.; Goeman, J. L.; Van der Eycken, J.; Boerjan, W.; Messens, E. *Plant Physiol.* **2004**, *136*, 4023−4036.
(39) Rohde, A.; Morreel, K.; Ralph, J.; Goeminne, G.; Hostyn, V.; De Rycke, R.; Kushnir, S.; Van Doorsselaere, J.; Joseleau, J. P.; Vuylsteke, M.; Van Driessche, G.; Van Beeumen, J.; Messens, E.; Boerjan, W. *Plant Cell* **2004**, *16*, 2749−2771.
(40) Ingalls, A. E.; Ellis, E. E.; Santos, G. M.; McDuffee, K. E.; Truxal, L.; Keil, R. G.; Druffel, E. R. M. *Anal. Chem.* **2010**, *82*, 8931−8938.
(41) Haupert, L. J.; Owen, B. C.; Marcum, C. L.; Jarrell, T. M.; Pulliam, C. J.; Amundson, L. M.; Narra, P.; Aqueel, M. S.; Parsell, T. H.; Abu-Omar, M. M.; Kenttämaa, H. I. *Fuel* **2012**, *95*, 634−641.
(42) Kawai, S.; Okita, K.; Sugishita, K.; Tanaka, A.; Ohashi, H. *J. Wood Sci.* **1999**, *45*, 440−443.
(43) Bozell, J. J.; O'Lenick, C. J.; Warwick, S. *J. Agric. Food Chem.* **2011**, *59*, 9232−9242.
(44) Long, W. J.; Mack, A. E. Comparison of Selectivity Differences Among Different Agilent ZORBAX Phenyl Columns using Acetonitrile or Methanol. http://www.chem.agilent.com/Library/applications/5990-4711EN.pdf (accessed Dec 26, 2011).
(45) Morreel, K.; Kim, H.; Lu, F. C.; Dima, O.; Akiyama, T.; Vanholme, R.; Niculaes, C.; Goeminne, G.; Inze, D.; Messens, E.; Ralph, J.; Boerjan, W. *Anal. Chem.* **2010**, *82*, 8095−8105.
(46) Antonio, C.; Larson, T.; Gilday, A.; Graham, I.; Bergstrom, E.; Thomas-Oates, J. *Rapid Commun. Mass Spectrom.* **2008**, *22*, 1399−1407.
(47) Amundson, L. M.; Eismin, R. J.; Reece, J. N.; Fu, M. K.; Habicht, S. C.; Mossman, A. B.; Shea, R. C.; Kenttämaa, H. I. *Energy Fuels* **2011**, *25*, 3212−3222.